Fourier Images : I—The Point Source

By J. M. COWLEY and A. F. MOODIE
Division of Industrial Chemistry, Commonwealth Scientific and Industrial Research Organization, Melbourne, Australia

Communicated by A. L. G. Rees; MS. received 4th April 1956

Abstract. The problem of designing a light or electron optical system specifically for the imaging of periodic objects, such as real crystals, is discussed. A qualitative appeal to communication theory suggests that it should be possible to devise systems of higher efficiency than the conventional microscope by using the *a priori* knowledge of periodicity.

The possibility of deforming the incident wavefront in such a way that the periodic object acts as its own imaging system is considered and a formalism is set up. The particular case of the spherical wavefront is then examined in detail and it is predicted that a new type of image should be formed on certain planes. Since this image is in many ways analogous to the Fourier projection of crystallography, and since it can only be formed by periodic objects, it is named the Fourier image.

Fourier images produced experimentally with light optics are presented and shown to be in agreement with theoretical predictions. Patterns on planes other than Fourier image planes are described briefly, but detailed treatment is deferred until Part II.

The possibility of application to the imaging of crystal lattices by electron optics is discussed, but a quantitative treatment of the crucial problems of finite source size and coherence are deferred until Part III.

§ 1. Introduction

Theoretical and experimental enquiry into the diffraction of transverse waves tends to fall into one of two distinct categories. The first includes investigations into the diffraction of non-planar waves by general objects, and the second the diffraction of planar waves by periodic objects. Consequently two quite separate approaches have been made to problems of image-formation; that of the microscopist, and that of the structure analyst.

When attempts are made to image molecules, severe difficulties are encountered in both techniques. In the former, the problem of the design of adequate electron lenses has yet to be solved, and in the latter, a particular solution of the phase problem virtually has to be obtained for every structure. Although structure analysis is both uncertain and extremely tedious, it has so far proved to be the only method capable of yielding a detailed molecular image. Thus the success of the technique has emphasized the extreme importance of the periodic object in optics, while the complexity of its procedures has demonstrated the desirability of developing a more direct method of imaging.

A considerable literature exists on the imaging of periodic objects in optical systems capable of imaging the general object (Abbe 1873, Hopkins 1953, Berek 1950) and recently there has been extensive discussion of novel methods for

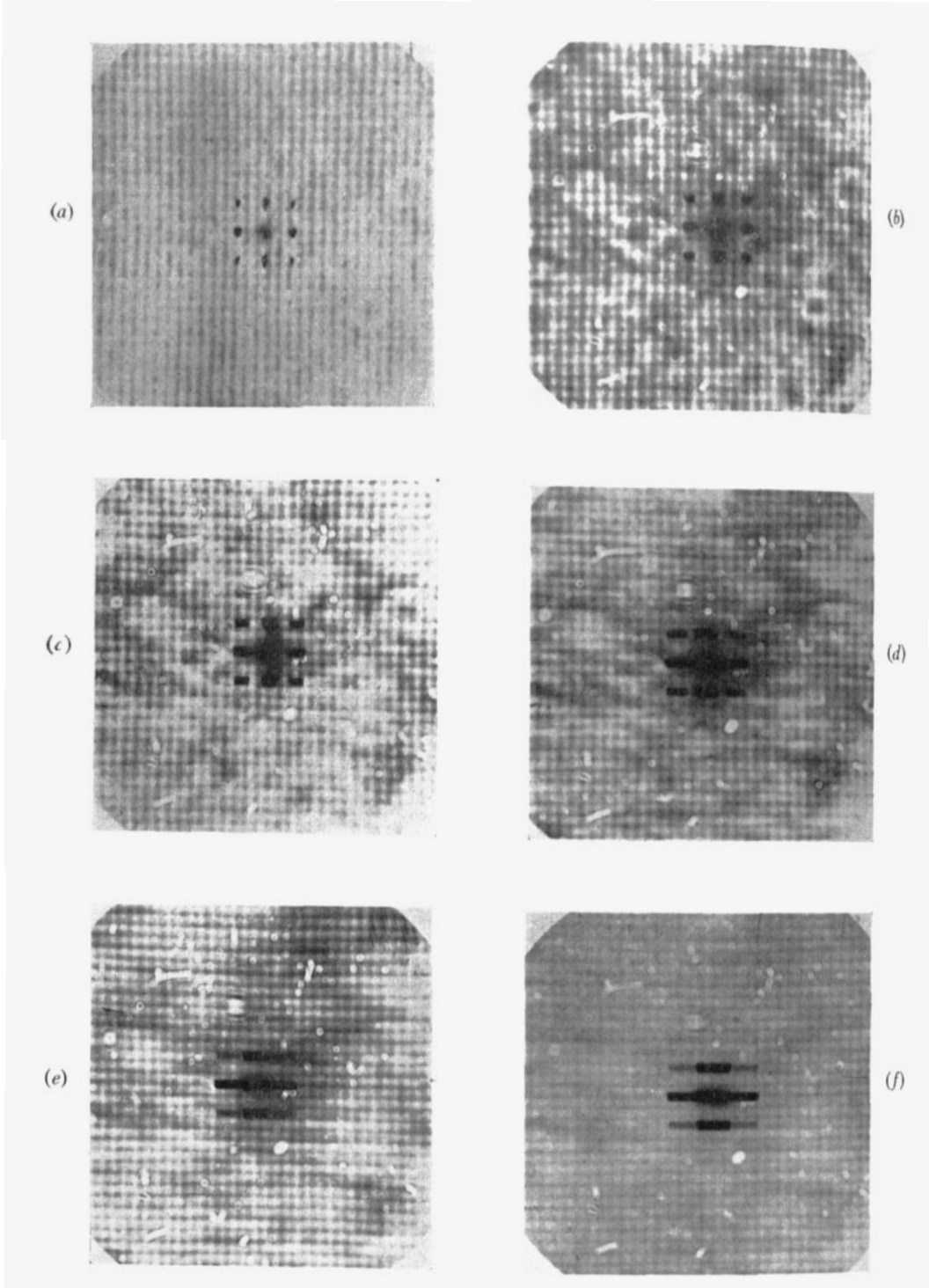

Figure 3. The $\nu = 2\frac{1}{2}$ Fourier images of maximum contrast, and the corresponding diffraction patterns, for a grating of 14·67 μ periodicity and a rectangular source of variable length. The photographs are taken with the variable source dimensions (*a*) 13 μ, (*b*) 40 μ, (*c*) 64 μ, (*d*) 93 μ, (*e*) 115 μ, (*f*) 136 μ.

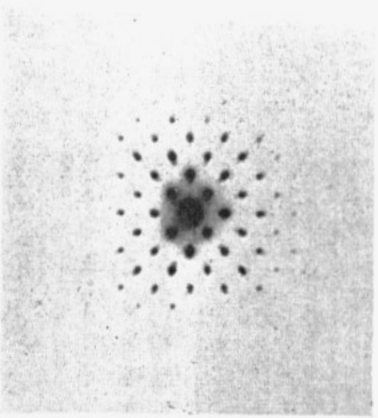

(*a*)

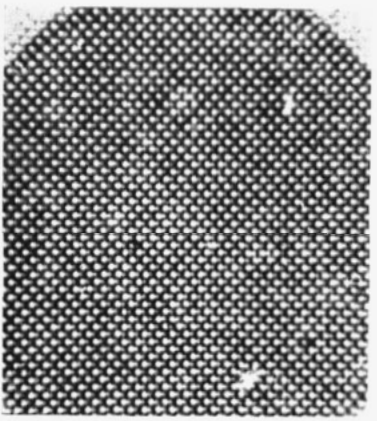

(*b*)

(*c*)

Figure 3. (*a*) Diffraction pattern obtained from the grating of figure 2; (*b*) Magnified image of the grating; (*c*) first Fourier image of the same grating. There is no trace of peak C of figure 2 (*b*).

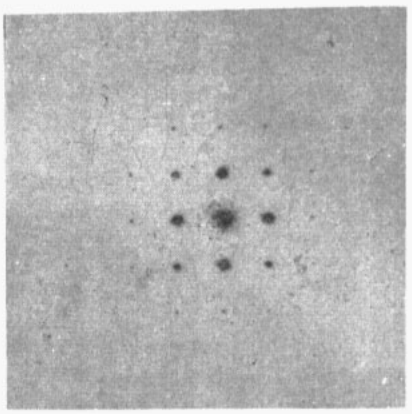

(*a*)

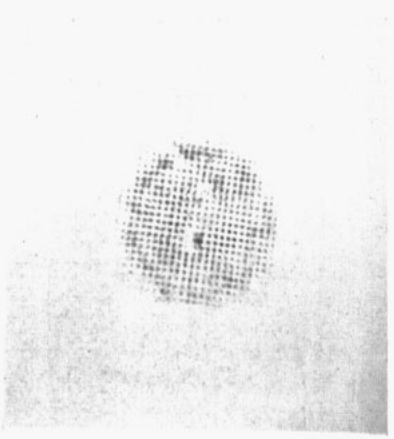

(*b*)

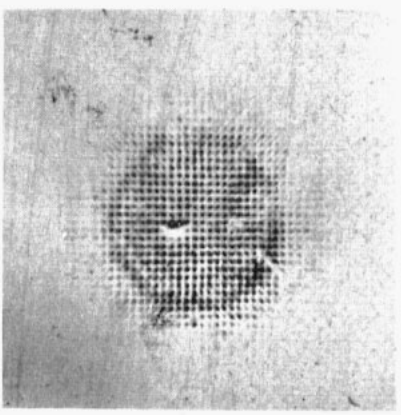

(*c*)

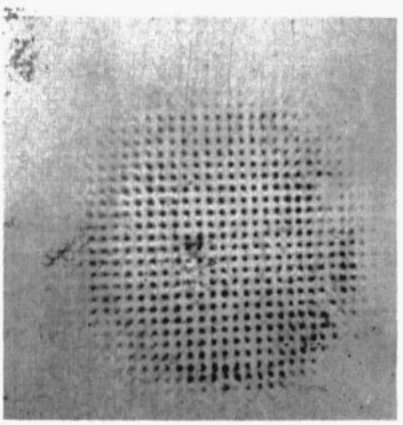

(*d*)

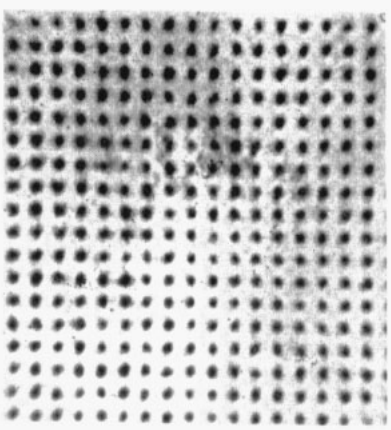

(*e*)

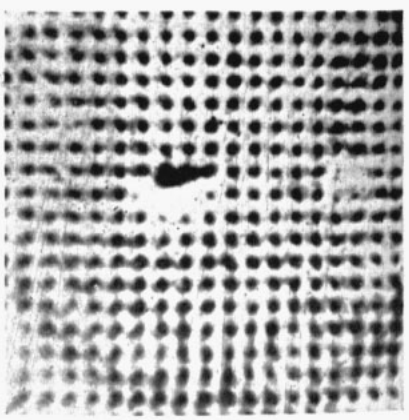

(*f*)

Figure 7. (*a*) $I(-\infty)$, the diffraction pattern; (*b*) $I(-\frac{1}{2})$, the first virtual Fourier image; (*c*) $I(0)$, the object; (*d*) $I(1)$; (*e*) $I(2)$; (*f*) Normal image of the same region at the magnification of $I(2)$.

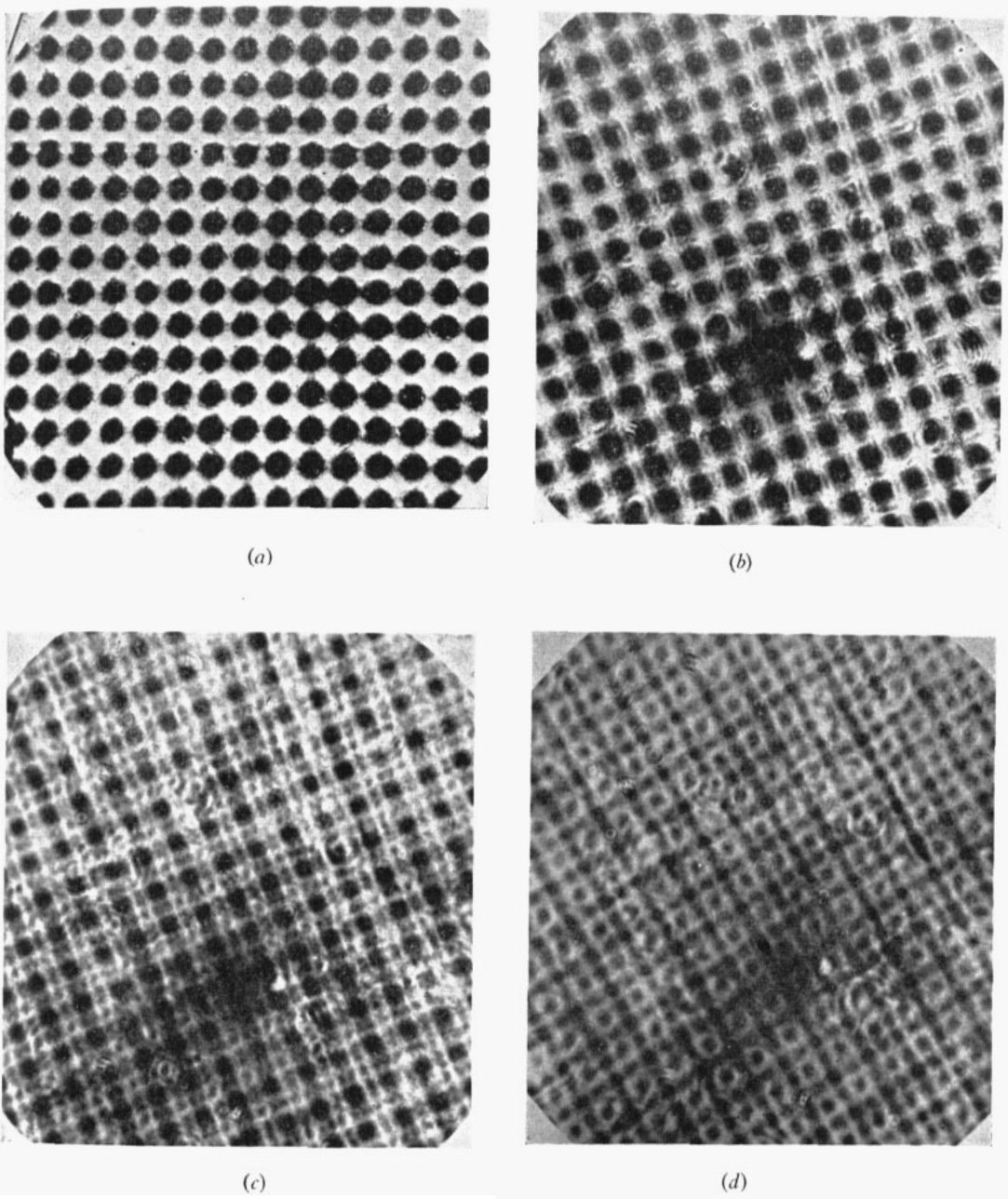

Figure 2 (*a*)-(*d*). Magnified image of periodic object. (*a*), $I(0)$; (*b*), $I(0{\cdot}075)$; (*c*), $I(0{\cdot}142)$; (*d*), $I(0{\cdot}204)$. See also Plate II.

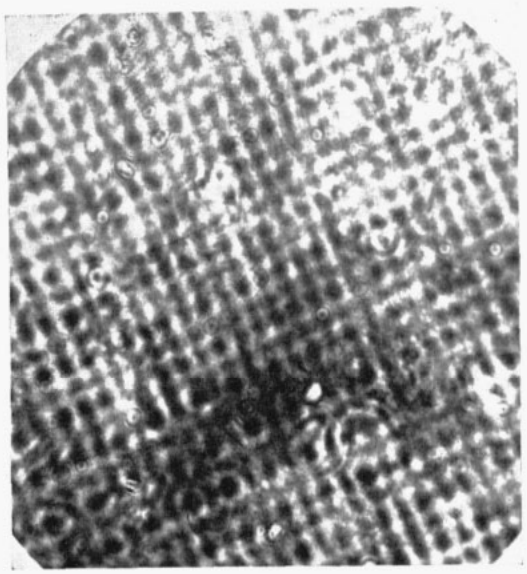

(*e*)

(*f*)

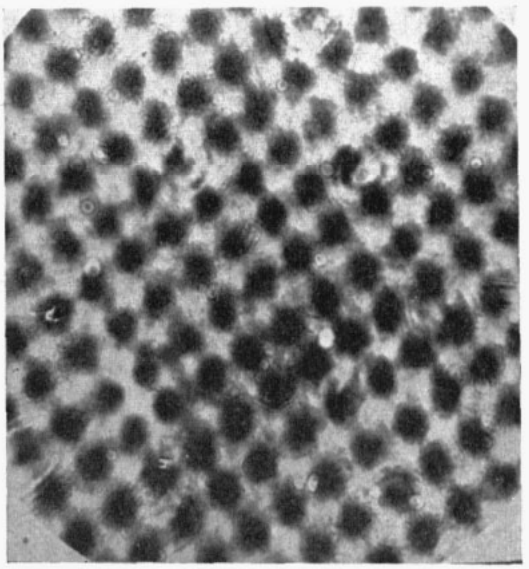

(*g*)

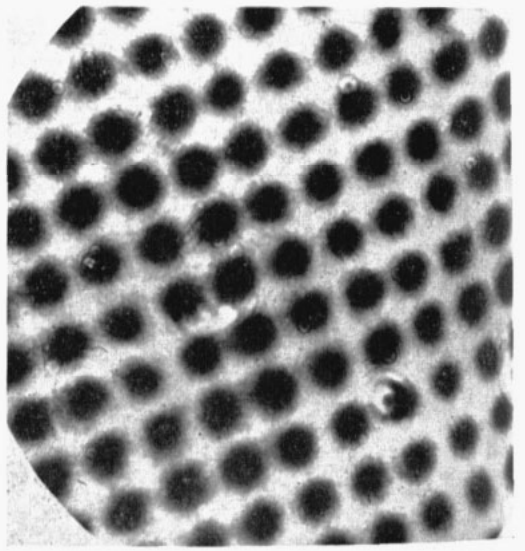

(*h*)

Figure 2 (*e*)–(*h*). Magnified range of periodic object. (*e*), I (0·258); (*f*), I (0·310); (*g*), I (0·363); (*h*), I (0·538).

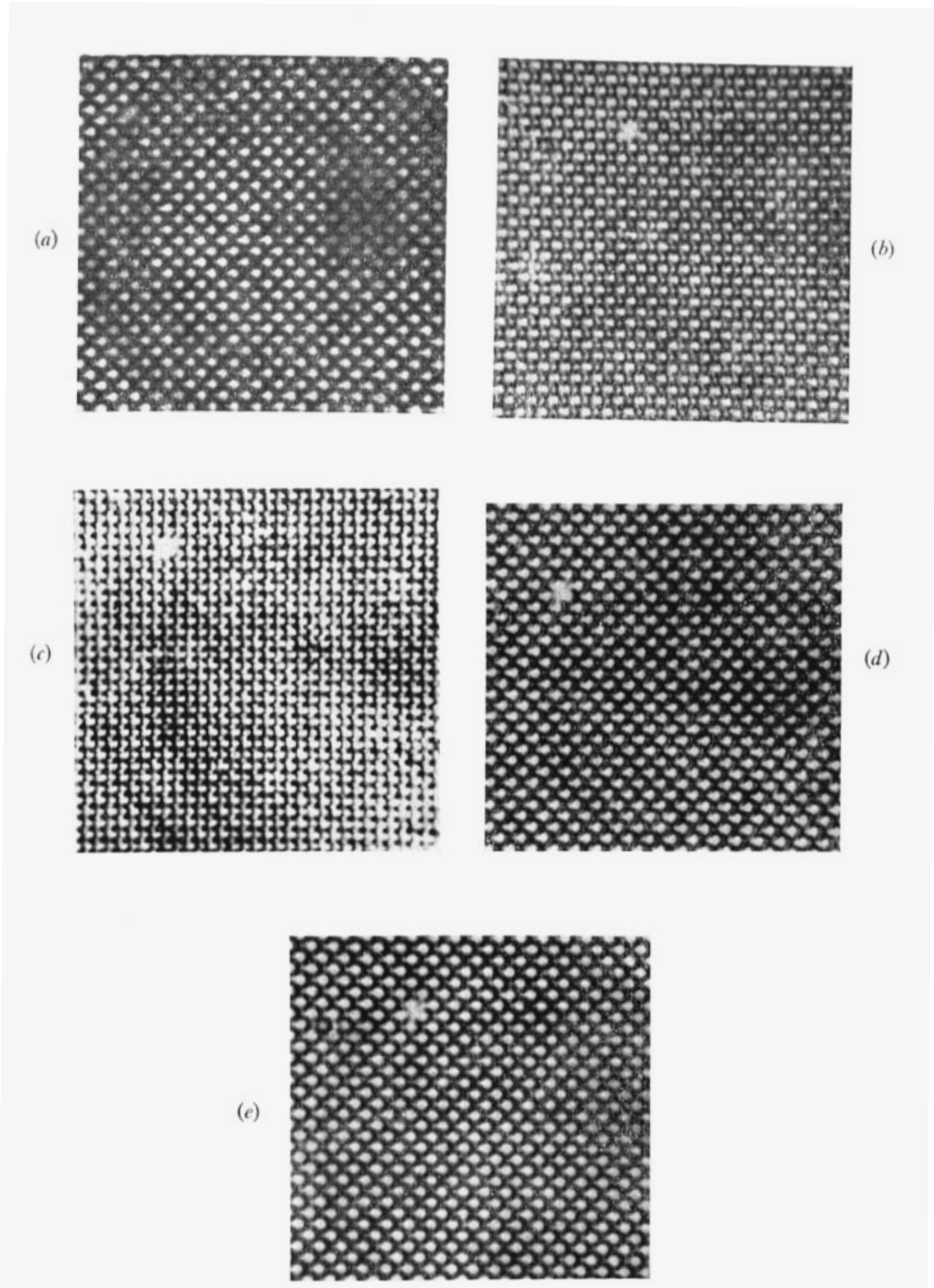

Figure 1. The $\nu = \frac{1}{2}$ Fourier images of an optical grating with 35·3 μ periodicity, obtained with two small sources separated, in a ' horizontal ' direction, by (*a*) 17 μ, (*b*) 46 μ, (*c*) 75 μ, (*d*) 110 μ, (*e*) 143 μ.

imaging general objects (Gabor 1949, 1951), but no consideration has been given to the problem of designing an optical system specifically for the imaging of periodic objects.

It is the purpose of the present series of papers to discuss one approach to this problem, and to present experimental evidence to show that under suitably restricted conditions periodic objects can be imaged by means of simple optical systems which do not include lenses or mirrors as essential components.

Communication theory offers many examples of the advantages to be gained by utilizing *a priori* information associated with a given system. While the precise relationship between communication filter theory and optics is a matter for debate, the two formalisms show marked similarities, and this has prompted a number of authors to investigate the possibility of adapting an imaging system to a particular class of objects (Blanc-Lapierre 1953, MacKay 1953). With the possible exception of the design of 'super-gain antennae', this idea has not found any considerable practical application. It does, however, have an important bearing on the present problem in that conventional systems do not exploit the *a priori* knowledge of periodicity. Thus the microscopist attempts to image the periodic object in a system capable of imaging the general object and the structure analyst deduces periodicity from his diffraction patterns. It is to be expected therefore, that if this *a priori* information could be exploited, a more efficient procedure would result. A system which achieved this might, for instance, possess the same resolving power as a real, conventional system, but employ simpler apparatus, or give higher resolution with apparatus of the same quality and complexity.

It is fundamental in image-forming systems that diffracted rays must be recombined with appropriate phase and amplitude. In enquiring into systems which might exploit periodicity, it is therefore natural at the outset to enquire whether the object itself can achieve this if a suitably shaped wavefront is incident upon it. Clearly an equi-path length condition cannot be satisfied, but the possibility of the practically equivalent condition of path lengths differing by an integral number of wavelengths may exist. It is then intuitively plausible that such a condition may obtain over a plane or planes with a spherical wavefront and a plane grating.

The immediate object of this paper is to examine the possibility of imaging a plane grating by means of a point source and to compare predictions with the relevant experimental results in light optics. Discussion of the limitations inherent to a real system, that is, of effectively finite sources, coherence and aberrations in any subsidiary optics, is deferred until later publications (Cowley and Moodie 1957a, b).

As can be appreciated from the following argument, the limitation to plane gratings need not, of itself, constitute a practical deterrent. An approximate statement of the condition that a real crystal should behave as a plane grating to a given wavelength is that the Ewald sphere should be substantially planar over a sufficiently large area in reciprocal space. This is not generally satisfied for X-rays of the wavelengths most commonly employed in structure determination, but is satisfied over a wide range of conditions for electrons in the energy ranges most frequently employed in microscopes and diffraction cameras. In other words, for a given setting of the crystal in the beam electrons of wavelengths in the region of 0·05 Å will produce a diffraction pattern which includes all of the orders associated

with an appropriate zone-axis, while x-rays of wavelength in the region of 1 Å will, in general, produce no pattern at all. Direct confirmation that sufficient structural information is available at one setting of the crystal to allow of precise determination of atomic positions has been obtained by one of the authors (Cowley 1953 a, b).

§ 2. Formal Statement of the Problem

The coordinate system of figure 1 is set up. In order to simplify the analysis the axes of the unit cell are chosen to be orthogonal. The transmission function of the general plane periodic object is then defined in the usual way by

$$\rho(\xi, \eta) = \sum_h \sum_k F_{hk} \cos 2\pi \left(h\frac{\xi}{a} + k\frac{\eta}{b} + \phi_{hk} \right) \qquad \ldots\ldots (2.1)$$

where (ξ, η) are direct lattice coordinates, (h, k) are reciprocal lattice coordinates and ϕ_{hk} are the phases associated with the structure amplitudes F_{hk}.

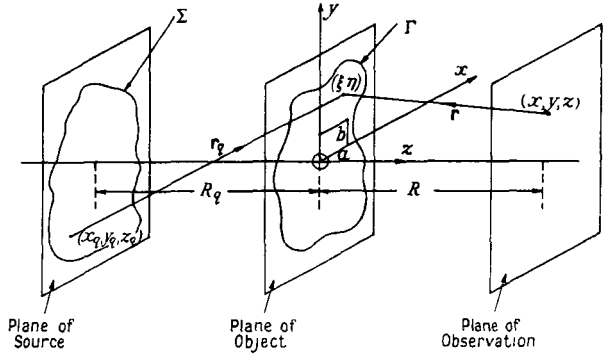

Figure 1. Coordinate system adopted in formal statement of the problem.

Suppose that the source lies on a plane parallel to the object plane and at a distance R_q from it, that (x_q, y_q, z_q) is a typical point on it, and that $\mathbf{r}_q$ is the vector from (x_q, y_q, z_q) to the point (ξ, η) on the object plane. Similarly, suppose that the plane of observation lies at a distance R from the object plane, that (x, y, z) is a point on it, and that $\mathbf{r}$ is the vector from (x, y, z) to (ξ, η).

If the source consists entirely of the point (x_q, y_q, z_q), and if the object consists of a screen with aperture Γ, then the wave function at (x, y, z) is given by the Kirchhoff integral,

$$v = \frac{1}{4\pi} \int_\Gamma (rr_q)^{-1} \left[\left(\frac{1}{r} + ik \right) \cos(\mathbf{n} \cdot \mathbf{r}) - \left(\frac{1}{r_q} + ik \right) \cos(\mathbf{n} \cdot \mathbf{r}_q) \right] \exp\{-ik(r + r_q)\}\, dS \qquad \ldots\ldots (2.2)$$

where dS is a surface element, $\mathbf{n}$ is the unit normal and $k = 2\pi/\lambda$.

The screen is now replaced by the periodic object $\rho(\xi, \eta)$ with bounds Γ and the source is described by a function $q(x_q, y_q)$ with bounds Σ. Then if dS_q is an element of surface on the source, the wave function at (x, y, z) is given by

$$u = \frac{1}{4\pi} \int_\Gamma \int_\Sigma \rho(\xi, \eta)\, q(x_q, y_q) (rr_q)^{-1} \left[\left(\frac{1}{r} + ik \right) \cos(\mathbf{n} \cdot \mathbf{r}) - \left(\frac{1}{r_q} + ik \right) \cos(\mathbf{n} \cdot \mathbf{r}_q) \right] \times \exp\{-ik(r + r_q)\}\, dS\, dS_q. \qquad \ldots\ldots (2.3)$$

For any source function, the evaluation of equation (2.3) is a formidable problem. Fortunately, under the experimental conditions envisaged, extensive

simplification is possible with negligible loss in accuracy. Thus both r and r_q will always be much greater than the wavelength and the maximum effective linear dimension of the object. Under these conditions (2.3) reduces to

$$u = \frac{\iota[\cos(\mathbf{n}\,.\,\mathbf{r}) - \cos(\mathbf{n}\,.\,\mathbf{r}_q)]}{2\lambda r r_q} \int_\Gamma \int_\Sigma \rho(\xi,\eta)\, q(x_q, y_q) \exp\{-ik(r+r_q)\}\, dS\, dS_q. \qquad \ldots\ldots(2.4)$$

Under equivalent conditions the approximation is better for electrons and a real crystal than for light and a true two-dimensional grating. Considerable use will be made of this fact since many steps in the analysis are purely formal and would be difficult to justify rigorously. The main justification will be sought in the quantitative comparison of theory with experiment. It will emerge that simple quantitative light optical tests are available for each main result, so that the experimentally much more involved electron-optical tests, in which the main practical interest lies, may be deferred with confidence.

§ 3. The Point Source and the Infinite Plane Periodic Object

The analysis will be made in one dimension. No new feature and no additional difficulty is encountered in two dimensions; the notation merely becomes more complicated. The results for two dimensions will be quoted at the end of the section.

A conventional parabolic approximation is made to $\exp\{-ik(r+r_q)\}$ so that

$$\exp\{-ik(r+r_q)\} = \exp\{-ik(b_0 + b_1\xi + b_2\xi^2)\} \qquad \ldots\ldots(3.1)$$

where $$b_0 = \tfrac{1}{2}\left(\frac{x_q^2}{R_q} + \frac{x^2}{R}\right);\ b_1 = -\left(\frac{x_q}{R_q} + \frac{x}{R}\right);\ b_2 = \tfrac{1}{2}\left(\frac{1}{R_q} + \frac{1}{R}\right).$$

Equation (2.4) then becomes

$$u = K_1 \int_{-\infty}^{\infty} \sum_h F_h \cos 2\pi\left(h\frac{\xi}{a} + \phi_h\right) \exp\{-ik(b_0 + b_1\xi + b_2\xi^2)\}\, d\xi. \qquad \ldots\ldots(3.2)$$

Reversing the order of integration and summation and then performing the integration,

$$u = K_1(1-i)\left(\frac{\pi}{2kb_2}\right)^{1/2} \exp\left\{ik\left(b_0 - \frac{b_1^2}{4b_2}\right)\right\} \sum_h \exp\{i\gamma_h^2\}\, F_h \cos 2\pi\left(\frac{h}{a}\,\frac{b_1}{b_2} - \phi_h\right) \qquad \ldots\ldots(3.3)$$

where $$\gamma_h^2 = \pi\lambda \frac{R+R_q}{RR_q}\,\frac{h^2}{a^2}.$$

The dependence of (3.3) on x_q is most conveniently displayed by rewriting it in the form

$$u = K_1(1-i)\left(\frac{\pi}{2kb_2}\right)^{1/2} \exp\{ik(c_0 + c_1x_q + c_2x_q^2)\} \sum_h \exp\{i\gamma_h^2\}\, F_h \cos 2\pi \times\left(E_h x_q + \frac{\psi_h}{2\pi}\right) \qquad \ldots\ldots(3.4)$$

where $$c_0 = R + R_q + \tfrac{1}{2}\frac{x^2}{R+R_q};\quad c_1 = -\frac{x}{R+R_q};\quad c_2 = \frac{1}{2(R+R_q)};$$

$$E_h = \frac{h}{a}\,\frac{R}{R+R_q};\quad \psi_h = 2\pi\left(\frac{R_q}{R+R_q}\,\frac{hx}{a} + \phi_h\right).$$

If the point source lies on the axis, i.e. $x_q = 0$, and if constant terms are gathered under K_2^2 the intensity at a point on the plane of observation is given by

$$I = uu^* = K_2^2 \left[\sum_h F_h^2 \cos^2 \psi_h + \sum_i \sum_j \cos(\gamma_i^2 - \gamma_j^2) F_i F_j \cos\psi_i \cos\psi_j \right]. \quad \ldots\ldots (3.5)$$

Suppose that it is possible to satisfy the set of conditions

$$\cos(\gamma_1^2 - \gamma_2^2) = \cos(\gamma_1^2 - \gamma_3^2) = \ldots = \cos(\gamma_i^2 - \gamma_j^2) = \ldots = +1. \quad \ldots\ldots (3.6)$$

Equation (3.5) then represents the intensity due to a distribution

$$\rho(x/M) = K_2 \sum_h F_h \cos\psi_h.$$

This distribution is identical with that of the original periodic object, but magnified by a factor

$$M = (R + R_q)/R_q. \quad \ldots\ldots (3.7)$$

This is the magnification that would be expected from a shadow image.

The conditions (3.6) in fact define a set of image planes. These conditions are equivalent to

$$\tfrac{1}{2} \frac{\lambda}{a^2} \frac{RR_q}{R+R_q} = \frac{m_{12}}{1^2 - 2^2} = \frac{m_{13}}{1^2 - 3^2} = \ldots = \frac{m_{ij}}{h_i^2 - h_j^2} = \ldots$$

where m_{ij} are a set of integers; or

$$\frac{1}{R} + \frac{1}{R_q} = \frac{1}{\nu} \frac{1}{2} \frac{\lambda}{a^2} \quad \ldots\ldots (3.8)$$

where ν is an integer, possibly negative. The system thus possesses multiple focal lengths $\nu(2a^2/\lambda)$.

Conditions equivalent to (3.8) in two dimensions are

$$\tfrac{1}{2}\lambda \frac{RR_q}{R+R_q} = \ldots = m_{ij} \left[\frac{(h_i^2 - h_j^2)}{a^2} + \frac{(k_i^2 - k_j^2)}{b^2} \right]^{-1}. \quad \ldots\ldots (3.9)$$

These conditions reduce to (3.8) provided

$$a/b = (n_1/n_2)^{1/2} \quad \ldots\ldots (3.10)$$

where n_1 and n_2 are integers.

The quantitative treatment of the patterns lying between the focal planes and the comparison of the theoretical and experimental results is somewhat lengthy. Further, the best approach differs considerably from that presented above. It is therefore proposed to defer this discussion to Part II of the series. For the purposes of the next section it is, however, necessary to consider one special case, that defined by

$$\frac{1}{R} + \frac{1}{R_q} = \frac{1}{\nu + \frac{1}{2}} \frac{1}{2} \frac{\lambda}{a^2}.$$

For such planes equation (3.5) becomes

$$I = K_2^2 \left[\sum_h F_h^2 \cos^2 \psi_h - \sum_i \sum_j F_i F_j \cos\psi_i \cos\psi_j \right].$$

This pattern is seen to result from the distribution

$$\rho\left(\frac{x}{M}\right) = \sum_h (-)^{|h|} F_h \cos 2\pi h \frac{x}{M} = \sum_h F_h \cos 2\pi h \frac{(x + \frac{1}{2})}{M}, \quad \ldots\ldots (3.11)$$

that is, from a distribution related to the original by a magnification and a translation of half the unit-cell edge.

Thus, focal planes exist whenever

$$\frac{1}{R} + \frac{1}{R_q} = \frac{1}{\nu}\frac{1}{2}\frac{\lambda}{a^2} \qquad \ldots\ldots(3.12)$$

ν being integral or half integral, positive or negative.

In order to distinguish between the conventional image and the patterns on the planes defined by (3.12) it is proposed to describe the former as images and the latter as Fourier images. The reasons for the choice of the word Fourier will appear later. It is further proposed to adopt the notation $I(\mu)$ for the pattern on the plane defined by (3.12) and with ν replaced by μ. Thus $I(3)$ refers to the sixth real Fourier image, and $I(8{\cdot}06)$ refers to the pattern on the plane defined by

$$\frac{1}{R} + \frac{1}{R_q} = \frac{1}{8{\cdot}06}\,\frac{1}{2}\,\frac{\lambda}{a^2}.$$

When all structure amplitudes except one are zero the conditions for focus disappear, so that a cosinusoidal grating is in focus for all R. The result for this special case has been derived by Gabor (1949) in the course of his investigations into the imaging of general objects.

Hopkins (1953), in considering the imaging of periodic objects by a lens, treated what was, in effect, the case of the gratings $\cos\theta$ and $1+\cos\theta$. For the latter it was found that multiple focal planes existed in the image space of the lens.

§ 4. Experimental

4.1. *Qualitative Observations*

With some care the phenomenon may be observed with a fine gauze and a distant light source. It is much simpler, however, to place the object on the stage of a microscope and use a pinhole and the substage condenser to form the source. On racking the objective up and down, a series of magnified and demagnified Fourier images are observed. The normal image plane, $I(0)$, may be identified on noting that only here do non-periodic objects such as specks of dust or flaws in the grating come into sharp focus. This 'filter-like' action is discussed in greater detail in Part II.

The origin of the focusing and magnification effects can be observed physically in the formation and interaction of Fresnel fringe patterns. On racking up the objective from its normal position, fringes are observed to run out from the detail in the image. Those originating from the periodic object reinforce to produce patterns of varying complexity. Finally they reinforce completely and a magnified image of the grating is formed. The cycle is repeated with increasing magnification and without loss of resolution. Beyond a certain point it is impossible to obtain a sharply focused image unless the crossover distance is set to satisfy the condition for focus at infinity, that is, $R_q = 2\nu a^2/\lambda$.

On racking the objective down from its normal position, a similar sequence is observed except that the Fourier images are virtual and reduced. The process begins to fail when the orders of diffraction fail to overlap completely, and terminates on the plane of the diffraction pattern. Here the objective is focused on the source.

The origin of the filter effect can be observed physically by repeating the above procedure, but this time confining attention to the non-periodic detail. Here again fringes run out from the objects on racking away from the normal position, but now, finding no corresponding fringes to interact with, they rapidly dissipate themselves, forming a background to the periodic component.

If the grating consists simply of two orthogonal sets of ruled lines, or of a gauze, these purely qualitative observations are not completely convincing. It has become almost conventional in investigations of this type to find that the Patterson function, or some closely related hybrid, is generated, and the reasons for this are usually elusive. Since the Patterson function of a grid, or a lattice consisting of a disc on the origin of the unit cell, bears a marked resemblance to the intensity distribution in the image itself, it is desirable to employ some more distinctive array for qualitative observations.

The authors are indebted to Mr. J. L. Farrant for making available to them a variety of gratings prepared by him in the course of a series of researches undertaken by Dr. A. L. G. Rees and himself on certain diffraction effects observed in the electron microscope. A sketch of the unit cell of one of these gratings is given in figure 2 (*a*), and a sketch of the essential features of the Patterson function of this cell in figure 2 (*b*). It will be noted that the presence or absence of peak C constitutes a test of whether a Patterson function or an image has been formed.

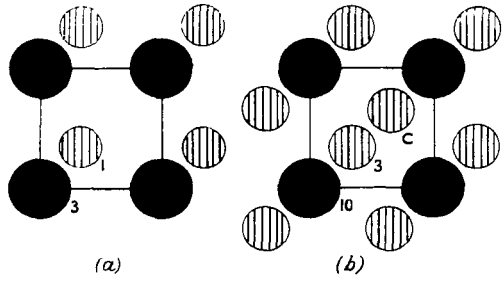

Figure 2 (*a*) Sketch of the unit cell of the grating employed to obtain figure 3 (*b*) Patterson function of (*a*). Approximate weights are indicated beside each peak.

Under conditions which will be described in § (4.2), the photographs of figure 3 (*a*), (*b*) and (*c*) (Plate) were obtained. Actual values used in the experiment were, $a = 35{\cdot}3\ \mu$, $R_y = 0{\cdot}545$ cm, $R = 0{\cdot}395$ cm, and $\lambda = 5461$ Å. Figure 3 (*b*) is the normal magnified image and figure 3 (*c*) is the Fourier image, $I(\frac{1}{2})$. It will be observed that, apart from a difference in magnification and a reduction in the resolution of non-periodic detail, the plates are identical. In particular, there is no trace of peak C. Qualitatively, then, at least, the image-like properties of these patterns predominate.

4.2. *Apparatus*

In order that the source to object distance may be readily varied, it is convenient to employ the reduced image of a pinhole as a source. Under these conditions Fourier image space can be divided into four distinct regions. This is illustrated in figure 4 for a divergent pencil incident on the object. In region I the Fourier images are real and magnified, in region II they are virtual and reduced, in region III they are virtual and reduced and in region IV they are virtual and magnified.

A corresponding set of regions exists for a convergent pencil incident on the object.

In order that all of these regions might be conveniently explored the experimental arrangement shown schematically in figure 5 was employed. A 60 watt mercury discharge lamp, a pinhole of approximately 1000 μ diameter, and a No. 77 Wratten filter formed the illuminating system for a Zeiss Opton microscope. Measurements along the optical axis could then be made with considerable precision by means of the calibrated fine focus control.

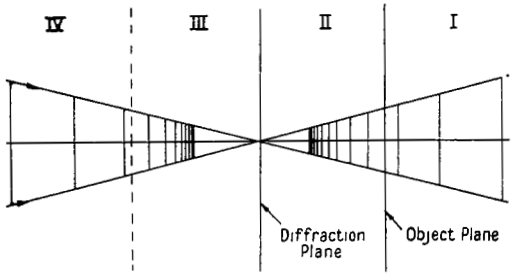

Figure 4. Distribution of Fourier image planes for a divergent pencil incident on the object

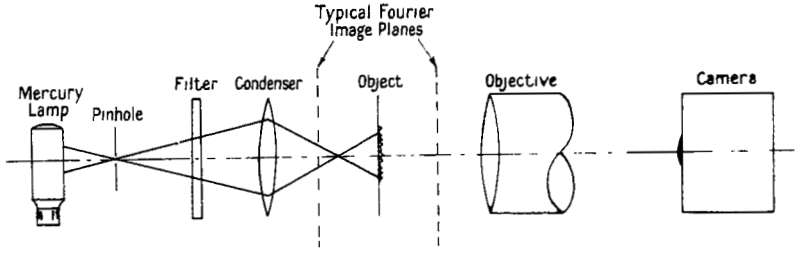

Figure 5. Experimental arrangement.

An effective source diameter of 30 μ was obtained with this system. While it might be considered that such an illuminating system by no means approximates to a point source when located only a few tenths of a millimetre from a grating of only 15 μ period, it was found that reduction of the diameter of the pinhole led to no change in the results within the limits of experimental error, but merely increased exposure times. The value given above was therefore adopted for experimental convenience. A quantitative discussion of this point, which turns out to be fundamental in the theory, is given, along with further experimental evidence, in Part III of this series.

Under these conditions exposures of approximately thirty minutes gave adequate density on Kodak Panatomic-X plates.

4.3. *Testing of Expressions for Location of Focal Planes and for Magnification*

In the experiments described in this section, a photograph of the reduced image of a gauze was employed as the periodic object. The length of the edge of the unit cell was found to be 14·67 $\mu \pm 0{\cdot}04\,\mu$ in the mean.

The distances R_q and R were found by focusing successively on the diffraction pattern, the object, and the relevant Fourier image plane. Measurements were

made for a range of values of R_q by varying the setting of the substage condenser.

The results of the measurements for both real and virtual images are compared with the calculated values in figure 6 (*a*) and (*b*). Theoretical and experimental values of the location of and the magnification on the set of Fourier image planes for which $R_q = 0{\cdot}226$ cm are compared in the table. Due to the limited traverse of the fine focus control, accuracy of measurement is low in this set. Nevertheless it can be seen that there is satisfactory agreement within the limits of experimental accuracy.

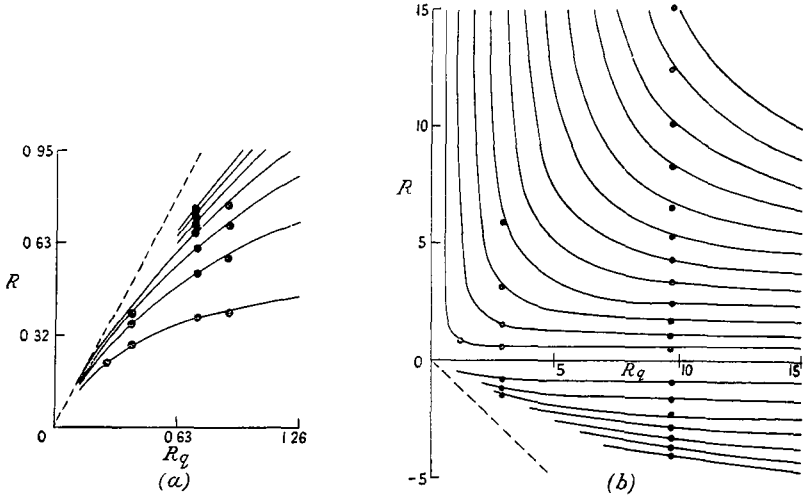

Figure 6 (*a*) Calculated and experimental locations of virtual Fourier image planes. (*b*) Calculated and experimental locations of real and virtual Fourier image planes for greater R_q. R and R_q are measured in units of $2a^2/\lambda$.

Comparison of the Theoretical and Experimental Values of the Location of and Magnification on a Series of Fourier Image Planes. $R_q = 0{\cdot}226$ cm. $a = 14{\cdot}67\,\mu$, $\lambda = 5461$ Å

	R_{calc} (cm)	R_{expt} (cm)	M_{calc}	M_{expt}
$-\frac{1}{2}$	−0·034	−0 033		
−1	−0 058	−0 056		
$-1\frac{1}{2}$	−0·078	−0·075		
−2	−0·093	−0 090		
$-2\frac{1}{2}$	−0·105	−0 103		
−3	−0·116	−0 115		
$-3\frac{1}{2}$	−0·124	−0·126		
$\frac{1}{2}$	0·048	0 048	1 21	1·20
1	0·121	0 119	1·52	1·51
$1\frac{1}{2}$	0·248	0 250	2 11	1 99
2	0·52	0 46	3·04	2 89
$2\frac{1}{2}$	1·54	1 13	6·00	5·70

A number of the patterns observed with this value of R_q, and reproduced in figure 7 (Plate), illustrate some of the reasons for choosing the term Fourier image.

It is clear from figure 7 (*c*), the object pattern, that the object deviates appreciably from ideal periodicity. Thus there is considerable local variation both in lattice parameter and in the shape of the constituent elements, together with a small regular increase in lattice parameter from the centre outwards, due to defects in the optical system employed in producing the grating.

All of these features will be reproduced in a conventional imaging system with an accuracy depending on the degree of perfection of the constituent optical components. The position is entirely different for Fourier images, and further, changes with the order of the image. This can be best appreciated by imagining R_q to be chosen so that the condition for focus at infinity is satisfied and by confining attention to local variations in lattice parameter and shape.

In $I(0)$, the pattern on the object plane, all variations are reproduced. In $I(\frac{1}{2})$, the first real Fourier image, only the Fresnel fringes from the periodic component have completely reinforced, while the fringes from the non-periodic component have already begun to dissipate. This may be regarded from a different point of view. The $|F_{hk}|$ decrease with distance from the origin of the reciprocal lattice. Hence in the lower order Fourier images, an averaging process takes place over only a limited number of the unit cells in the object.

As the order-number of the Fourier image increases Fresnel fringes originating from the non-periodic component are increasingly dissipated, or alternatively, the averaging takes place over an increasing number of unit cells. Finally, in $I(\infty)$, the average pattern over the whole grating is reproduced in the same way as in a Fourier projection or section calculated from the integrated intensities of the diffraction pattern.

This conception of averaging is familiar in structure analysis where a real effectively infinite crystal is regarded formally as an ideal effectively infinite crystal convoluted with an appropriate modification function. The structure amplitudes of the real crystal may then be regarded as the product of the structure amplitudes of the ideal crystal and the Fourier transform of the modification function. It is usual to treat temperature effects in this way. Thus the pattern shown in figure 7 (*a*) might be described as one having a high temperature factor, since the intensity falls off rapidly with increase in reciprocal lattice coordinate. It would therefore be expected that $I(\infty)$ would exhibit relatively poor definition in this particular case, certainly considerably poorer than $I(0)$. The expected loss in definition is however seen to follow entirely from deficiencies in the object and not in the system. In fact, under these circumstances, loss in definition might be taken as a measure of the efficiency of the system.

On examining figure 7 it is, in fact, observable that the Fourier images approach the mean with increasing order number.

An isolated object constitutes an extreme case of this local variation. As can be seen such an object is sharply focused in $I(0)$, but has virtually disappeared in $I(2)$.

§ 5. Discussion

The most obvious aspects of the limited theory presented here seem to be well substantiated experimentally for light optics.

The principal interest, however, lies in electron optics, where on a first inspection it would appear that even better agreement could be expected. Thus, for practical orders of magnitude the approximation of equation (2.4) holds more accurately for electrons than for photons. Further, electron sources of much

greater intensity than light sources are readily available, and the limiting factor in resolution appears to be the perfection of the object. This latter is much lower for an optical grating than for most crystalline substances.

The effects of finite source size and the closely related subject of coherence, however, emerge as the crucial factors in considerations of application to practical electron-optical systems. These subjects are considered quantitatively in Parts II and III of this series and further discussion of application is therefore deferred to those papers.

References

Abbe, E., 1873, *Arch. mikrosk Anat.*, **9**, 431.

Berek, M., 1950, *Optik*, **6**, 1.

Blanc-Lapierre, A., 1953, *Communication Theory*, Edited by Willis Jackson (London Butterworths Scientific Publications)

Cowley, J. M., 1953 a, *Acta Cryst., Camb.*, **6**, 516; 1953 b, *Ibid.*, **6**, 522

Cowley, J. M., and Moodie, A. F., 1957 a, *Proc. Phys. Soc* B, **70**, 497; 1957 b, *Ibid*, **70**, 505.

Gabor, D., 1949, *Proc Roy Soc.* A, **197**, 454; 1951, *Proc Phys Soc.* B, **64**, 449

Hopkins, H. H., 1953, *Proc. Roy Soc* A, **217**, 408.

MacKay, D. M., 1953, *Communication Theory*, Edited by Willis Jackson, p. 521 (London Butterworths Scientific Publications).